Supporting information:

Enhancing the efficiency and stability of perovskite solar cells based on moisture-resistant dopant free hole transport materials by using 2D-BA_2PbI_4 interfacial layer

Farzaneh S. Ghoreishi [a,b], *Vahid Ahmadi* [a,c,*], *Maryam Alidaei* [c], *Farzaneh Arabpour Roghabadi* [c,d], *Mahmoud SamadPour* [e], *Reza Poursalehi* [a], *Erik M. J. Johansson* [b]

[a] Department of Nanotechnology Engineering, Tarbiat Modares University, Tehran, 14115-111, Iran
[b] Department of Chemistry—Ångström-Laboratory, Institution of Physical Chemistry, Uppsala University, Uppsala, 75120-523, Sweden
[c] Department of Electrical & Computer Engineering, Tarbiat Modares University, Tehran, 14115-194, Iran
[d] Department of Chemical Engineering, Tarbiat Modares University, Tehran,14115-114, Iran
[e] Department of Physics, K.N. Toosi University of Technology, Tehran, 15418-49611, Iran

* *Corresponding Author:* v_ahmadi@modares.ac.ir

Since the thickness of the 2D interfacial layer affects some properties in the PSCs such as charge transportation, hysteresis, etc., this parameter is optimized by using different concentrations for BAI solution. We have used BAI solutions with a concentration of 5 mg/ml, 10 mg/ml and 15 mg/ml while the spin coating parameters were fixed. Photovoltaic parameters for devices fabricated with three different concentrations for BAI solutions and with TQ1 and P3HT HTLs are presented in Table. S1. As can be seen clearly the best results are related to the cells with 10 mg/ml BAI solution. So, we applied this optimized value to the rest of our devices.

Table. S1. Photovoltaic performance of PSCs with three different concentrations for BAI solution as the precursor for the BA_2PbI_4 interfacial layer.

Device	Voc (V)	Jsc (mA/cm^2)	FF	η (%)
MAPI/BA_2PbI_4 (5 mg/ml)/TQ1	0.94	19.6	0.64	11.81
MAPI/BA_2PbI_4 (10 mg/ml)/TQ1	0.92	20.7	0.62	11.85
MAPI/BA_2PbI_4 (15 mg/ml)/TQ1	0.92	20.1	0.62	11.58
MAPI/BA_2PbI_4 (5 mg/ml)/P3HT	0.99	21.9	0.68	14.88
MAPI/BA_2PbI_4 (10 mg/ml)/P3HT	1.01	21.4	0.69	14.97
MAPI/BA_2PbI_4 (15 mg/ml)/P3HT	0.97	22.2	0.68	14.65

The EDX mapping analysis for the multi-layers with FTO/TiO_2/MAPI/BA_2PbI_4 structure is shown in Figure.S1. The cross-sectional FESEM image of the substrate with mentioned layers and the amount of different elements in them can be seen in this Figure. As we know, both 3D (MAPI) and 2D perovskites (BA_2PbI_4) contain organic precursors that contain carbon and nitrogen. Also due to the structure of BAI which is composed of phenyl rings, so there might be errors in the EDX mapping. Another concern is related to the diffusion of the electronic beam during the mapping analysis. Since this value is almost higher than the thickness of the layers, the position of each element marked by EDX mapping cannot be distinguished for each layer.

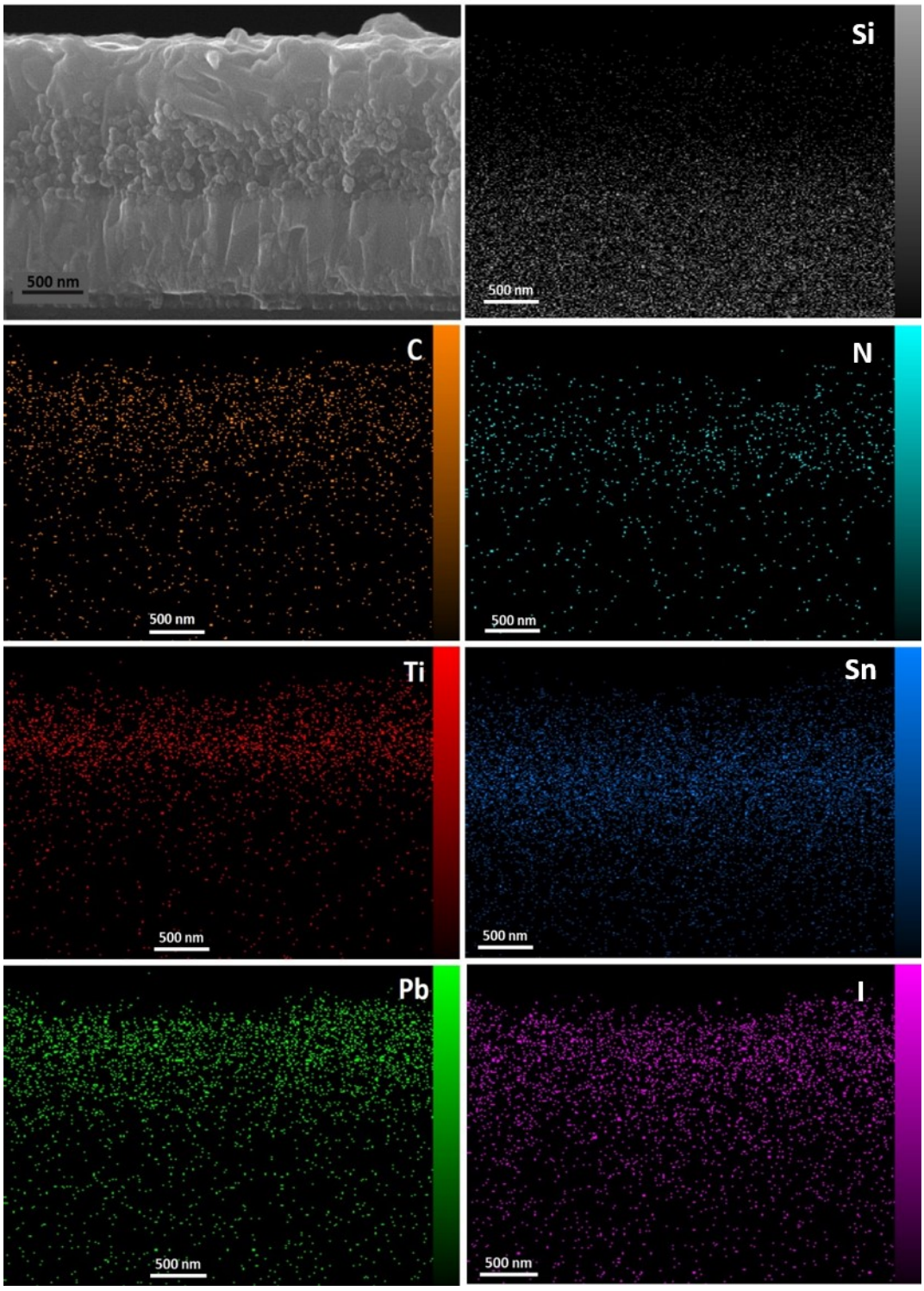

Fig. S1. EDX mapping analysis of the substrate with FTO/TiO_2 /MAPI/BA_2PbI_4 configuration. The cross-sectional FESEM image of these layers and also the amount of different elements in these layers are shown.

The photovoltaic parameters of 20 cells for each structure (MAPI/TQ1, MAPI/P3HT, MAPI/BA_2PbI_4/TQ1 and MAPI/BA_2PbI_4/P3HT) are obtained with a fixed scan rate of 50 mV/s and the corresponding statistical histograms of the PCE, FF, V_{OC} and J_{SC} are presented in Fig. S2(a)-(d), respectively. The average photovoltaics parameters of fabricated devices are also summarized in Table. S2.

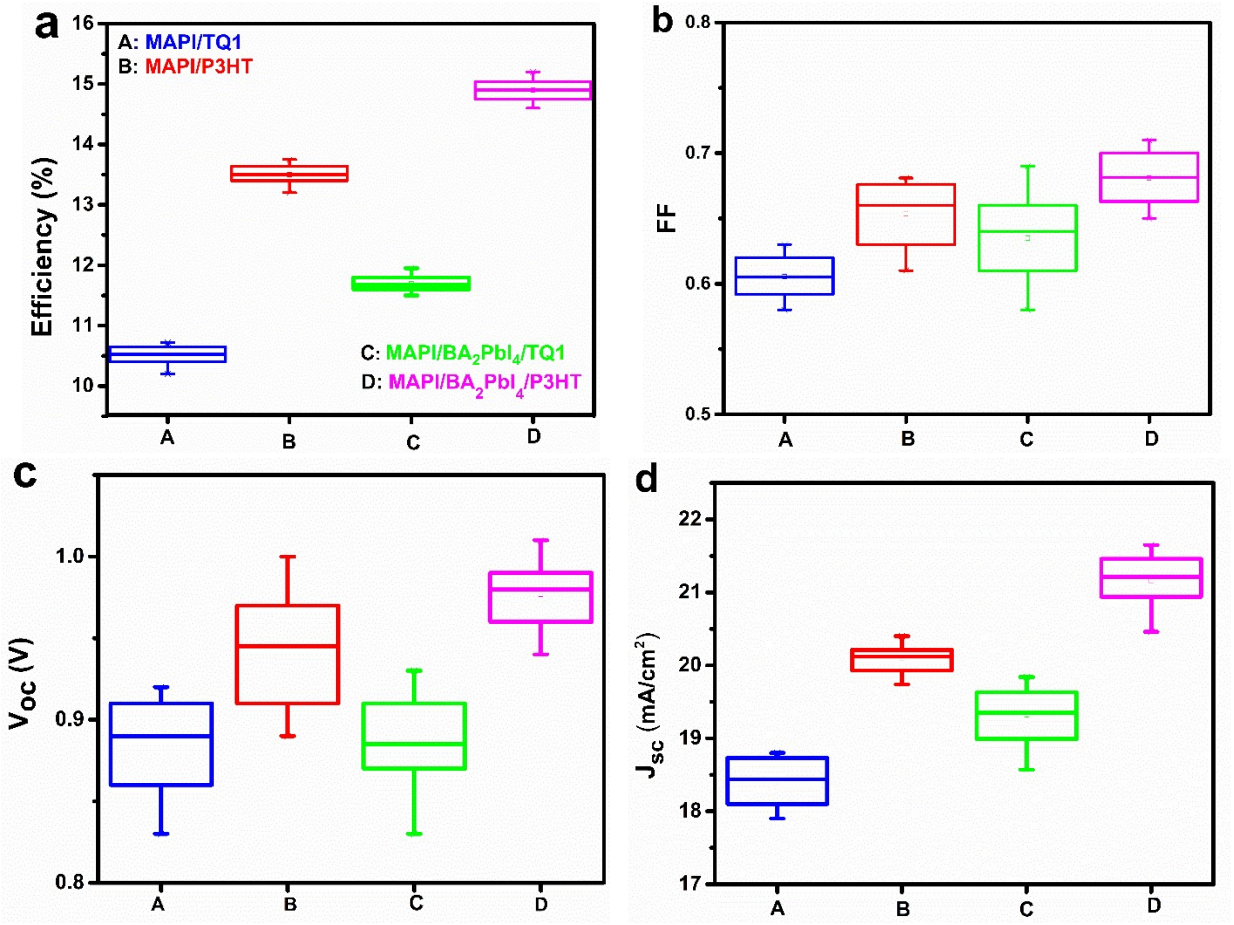

Fig. S2. Statistical histograms of the (a) PCE, (b) FF, (c) V_{OC} and (d) J_{SC} for MAPI/TQ1(A), MAPI/P3HT (B), MAPI/BA_2PbI_4/TQ1 (C) and MAPI/BA_2PbI_4/P3HT (D) based devices measured from 20 cells.

Table. S2. Average photovoltaics parameters of fabricated devices with and without interface modification and with TQ1 and P3HT HTLs.

	MAPI/TQ1	MAPI/P3HT	MAPI/BA_2PbI_4/TQ1	MAPI/BA_2PbI_4/P3HT
PCE (%)	10.52	13.51	11.75	14.9
Voc (V)	0.88	0.95	0.89	0.98
Jsc(mA/cm^2)	18.4	20.11	19.4	21.23
FF	0.61	0.66	0.64	0.68

Table. S3 shows the fitting parameters for MAPI/TQ1, MAPI/BA2PbI4/TQ1, MAPI/P3HT and MAPI/BA_2PbI_4/P3HT perovskite cells by the equivalent circuit model which is shown in the inset of Fig. 6(a). Nyquist plots and fitting graphs are represented in Fig. 6(a)-(d). Here, R_s is the series resistance, C_1 and R_1 are associated with the high-frequency arc in the Nyquist plot. C_1 is the geometric capacitance of the perovskite layer, and it can also contain the components of the contact layers. [1] R_1, the transport resistance, could be ascribed to the conductivity of the perovskite layer. On the other hand, it has been shown that R_1 could clearly be affected by the transport resistance of HTL. [1-3] C_2 and R_2 are the capacitance and resistance in the mid-frequency range, which are dependent on the contact properties. It is believed that mid-frequency features are related to the electronic surface states at interfaces but need more investigation. [1-4] C_3 and R_3 are the capacitance and resistance in the low-frequency domain of the complex impedance plane. C_3 is determined by the ionic and electronic charge accumulation at the electrode interfaces. R_3 is the recombination resistance at the perovskite/contact interfaces, [1, 5, 6] and also the inductive feature is specified by L in the equivalent circuit model. [7]

Table.S3. Fitting parameters for MAPI/TQ1, MAPI/BA_2PbI_4/TQ1, MAPI/P3HT and MAPI/BA_2PbI_4/P3HT perovskite cells by the equivalent circuit model which is shown in the inset of Fig. 6 (a).

Fitting parameters	R_s (Ω)	CPE_2-T	CPE_2-P	R_2 (Ω)	CPE_3-T	CPE_3-P	R_3 (Ω)	L (mH)	R_1 (Ω)	CPE_1-T	CPE_1-P
MAPI/TQ1	17.13	7.86E-05	0.59	56.77	0.66E-3	0.55	355.9	0	253	6.90E-08	0.87
MAPI/BA_2PbI_4 /TQ1	16.3	5.17E-06	0.67	1230	5.02E-5	0.58	1000	735.5	94.09	6.62E-08	0.90
MAPI/P3HT	19.8	4.24E-06	0.99	7.834	0.17E-3	0.61	199.8	0	153.2	4.47E-08	0.94
MAPI/BA_2PbI_4 /P3HT	15.6	1.77E-05	0.59	283.8	7.41E-5	0.68	426.4	56.72	130.8	4.37E-07	0.80

References

1. A. Guerrero, G. Garcia-Belmonte, I. Mora-Sero, J. Bisquert, Y. S. Kang, T. J. Jacobsson, J.-P. Correa-Baena and A. Hagfeldt, *J. Phys. Chem. C*, 2016, **120**, 8023-8032.
2. A. Krishna, D. Sabba, H. Li, J. Yin, P. P. Boix, C. Soci, S. G. Mhaisalkar and A. C. Grimsdale, *Chem. Sci.*, 2014, **5**, 2702-2709.
3. H. Li, K. Fu, P. P. Boix, L. H. Wong, A. Hagfeldt, M. Grätzel, S. G. Mhaisalkar and A. C. Grimsdale, *ChemSusChem*, 2014, **7**, 3420-3425.
4. J. Bisquert, G. Garcia-Belmonte, Á. Pitarch and H. J. Bolink, *Chem. Phys. Lett.*, 2006, **422**, 184-191.
5. A. Dualeh, T. Moehl, N. Tétreault, J. Teuscher, P. Gao, M. K. Nazeeruddin and M. Grätzel, *ACS Nano*, 2014, **8**, 362-373.
6. L. N. Quan, M. Yuan, R. Comin, O. Voznyy, E. M. Beauregard, S. Hoogland, A. Buin, A. R. Kirmani, K. Zhao and A. Amassian, *J. Am. Chem. Soc.,* 2016, **138**, 2649-2655.
7. H. D. Pham, S. M. Jain, M. Li, S. Manzhos, K. Feron, S. Pitchaimuthu, Z. Liu, N. Motta, H. Wang and J. R. Durrant, *J. Mater. Chem. A.*, 2019, **7**, 5315-5323.